Density dependent groundwater flow near deepwell infiltration systems, Modelling aspects

J.M. van Esch
Delft Geotechnics, P.O. Box 69, 2600 AB Delft, The Netherlands
Delft University of Technology, P.O. Box 5048, 2600 GA Delft, The Netherlands

A. Stakelbeek
Water Supply Company of North Holland, P.O. Box 5, 2060 BA Bloemendaal, The Netherlands

In this article a coupled flow-transport model is presented by which the time dependent behaviour of the brackish zone between salt and fresh groundwater can be simulated. The model will be used to optimize the balance between groundwater infiltration and abstraction as it takes place in deepwell infiltration systems, under the restriction that low concentration of salt makes the abstracted water useless for drinking water production. Although it can be shown that the model presented here gives promising results, it has to be adjusted to be useful in engineering practice. Some suggestions are given to reduce computational time and use of memory.

Introduction

The dune area along the North sea coast in the north-western part of the Netherlands is one of the most valuable natural areas in this country. To keep the groundwater, for ecological reasons, at an adequately high level, groundwater abstraction has been reduced in the last 30 years from about 20 Mm^3/year to about 2 Mm^3/year. This reduction of the abstraction of natural groundwater has been compensated by an artificial recharge system, which has become the predominant production method in the western part of Holland. Particularly the method of deep-well infiltration is winning ground because its slight spacial demands combined with small eco-hydrological impact.

PWN, Water Supply Company of North Holland, has been operating a deep-well infiltration system since the beginning of 1990. Its capacity is 5 Mm^3/year. The infiltration is carried out by means of 20 infiltration wells into an aquifer 50 to 100 metres below sea level. Abstraction is carried out by 12 abstraction wells in the same aquifer in which the infiltration wells are situated. This semi-confined aquifer is bounded at the lower side by a thin silty layer, under which the groundwater is brackish. An overinfiltration of 10% is maintained to avoid upconing of the brackish groundwater under the abstraction wells. Salt concentrations higher than 200 mg/l make the abstracted water unsuitable for drinking water production.

Recently a research project has been started for the development of a numerical model, by which low salinities can be predicted for this really three dimensional and time dependent problem. The model will be calibrated by hydraulic head measurements and resistivity measurements of electrode cables which are placed under the abstraction wells and in infiltration wells at several locations. The model will be used to optimize the balance between infiltration and abstraction. Further an estimation can be made of the length of the period the groundwater abstraction can be continued, when the infiltration is interrupted in the case of a calamity. If this period turns out to be sufficient long then the deep-well infiltration system will be an important reserve storage, when the surface water used for infiltration is polluted.

Basic equations

In this paragraph the main equations that form the coupled flow-transport model will be given by which the time dependent behaviour of the brackish zone can be simulated. For it is assumed that the equations are known to most of the readers, the equation will be presented in a short form, for details see [Bear 1972 and Bear Verruijt 1987].

The flow equation follows from Darcy's law and continuity of mass:

$$\frac{\partial(\rho n)}{\partial t} = \rho(\alpha+n\beta_p)\frac{\partial p}{\partial t}+\rho n\beta_c\frac{\partial c}{\partial t} = \nabla\cdot\left(\frac{\rho K}{\mu}\cdot(\nabla p+\rho g)\right) \qquad (1)$$

where the pressure p is the basic variable. The time dependent terms are all on the left hand side, ρ represents the fluid density, n is the porosity of the soil matrix and t is the time. The coefficient α accounts for the deformation of the solid matrix and follows from a linear state equation $\alpha = dn/dp$. The β_p coefficient accounts for the compression of the fluid and follows from the state equation $\beta_p = 1/\rho\cdot\partial\rho/\partial p$. The coefficient β_c describes the relation $\beta_c = 1/\rho\cdot\partial\rho/\partial c$. At the right-hand side K is the second-order intrinsic permeability tensor, μ is the dynamic viscosity and **g** the gravity constant.

The mass-transport equation, where the salt concentration c is the basic variable, reads:

$$R\frac{\partial c}{\partial t} = -\nabla\cdot(vc)+\nabla\cdot(\boldsymbol{D}\cdot\nabla c) \qquad (2)$$

where R is called the retardation factor due to adsorption, which assumes a constant state of equilibrium between the concentration in the fluid c and the concentration at the solid matrix c'. The partitioning coefficient between these concentrations is called the linear equilibrium isotherm $K = c'/c$. The retardation factor can be written as: $R = 1 + (1-n)/n\cdot K$. The first term at the right hand side represents the transport by convection, v is the real pore velocity vector of the fluid. The second term represents the dispersion part, where **D** is the second order dispersion tensor.

The fluid velocity in the pores follows from the Darcy velocity and is written as:

$$v = -\frac{K}{n\mu}\cdot(\nabla p+\rho g) \qquad (3)$$

For an isotropic medium the dispersion tensor equals:

$$\boldsymbol{D} = (d+\alpha_t|v|)\boldsymbol{I}+(\alpha_l+\alpha_t)\frac{vv^T}{|v|} \qquad (4)$$

The unit tensor is denoted by **I**, d represents the molecular diffusion coefficient. The two parameters α_l and α_t in this expression are the longitudinal and transverse dispersivity, respectively. In a homogeneous medium they both are of the order of the pore size. For a practical situation the dispersivities are dominated by variations in the velocity field, mainly due to variations in the intrinsic permeability field. Both the velocity field and the dispersion field can be calculated from the flow equation. The longitudinal dispersivity is usually much larger than the transverse dispersivity.

For the case of coupled flow the fluid density and fluid viscosity are assumed to be some function of the pressure and the concentration.

The state equation $\rho = \rho(p,c)$ linearized around the point $\rho_0 = \rho(p_0,c_0)$ for the fluid density is written as:

$$\rho = \rho_0\{1+\beta_p(p-p_0)+\beta_c(c-c_0)\} \tag{5}$$

where ρ_0 is a reference value for the fluid density at pressure p_0 and concentration c_0. The coefficients β_p and β_c indicate the change in fluid density as a function of pressure and concentration, respectively. The coefficients are defined by $\beta_p = 1/\rho \cdot \partial\rho/\partial p$ and $\beta_c = 1/\rho \cdot \partial\rho/\partial c$.

The state equation for the dynamic fluid viscosity $\mu = \mu(p,c)$ is linearized in the same manner, leading to:

$$\mu = \mu_0\{1+\gamma_p(p-p_0)+\gamma_c(c-c_0)\} \tag{6}$$

where μ_0 is a reference value for the viscosity at pressure p_0 and concentration c_0. The coefficients γ_p and γ_c specify the change in viscosity relative to the pressure and concentration change and are defined by $\gamma_p = 1/\mu \cdot \partial\mu/\partial p$ and $\gamma_c = 1/\mu \cdot \partial\mu/\partial c$.

Equations 1 to 6 form the coupled flow-transport model. A unique solution for a practical problem can be found under specific initial and boundary conditions.

Numerical model

The solution of equations 1 and 2 is approximated by the finite element method. According to this method the computational domain is subdivided in a large number of elements. The basic variables (pressure and concentration) are calculated in the nodal points of the mesh. Inside the element the values of these variables can be obtained by interpolation using the shape function. In this paper isoparametric 4 nodded quadrilateral and 8 nodded hexahedral elements are used, for 2D and 3D simulations respectively. Soil properties are taken constant within an element, the mesh is fixed in space (Eulerian description) which seems to be physically reasonable. Velocity vectors and dispersion tensor values are computed in the interpolation points, (Gauss points).

A sequential solution scheme is employed for solving the sets of equations 1 and 2 [Huyakorn and Pinder 1983]. At first the flow equation is solved using an estimate of the concentration field. Then the mass equation is solved using the computed velocity field. This procedure is repeated for the same time increment until concentration and pressure stabilize. The numerical formulation for both sets of equations is found using the Galerkin formulation [Bathe 1996 and Zienkiewics 1977]. The Galerkin method is a special case of the method of weighted residuals where the weight functions are chosen equal to the shape functions.

A consistent formulation for the flow equation has been found by order reduction of the gravitation field. A lumped mass formulation has been employed to increase the stability of the mass transport equation. The set of linear equations for pressures has a sparce symmetric coefficient matrix and is solved by the ordinary conjugate gradient method [Press ea., 1988]. The second set contains a sparce but asymmetric matrix of coefficients and is solved using the biconjugate gradient method.

Preliminary results

As a demonstration some simulation results are shown in figures 1 to 5. In these figures iso-concentration lines are drawn, the upmost isoline corresponds to a concentration 0.1, the lowest line corresponds to a concentration 0.9. The problem concerns a homogeneous layer with a source

of 0.33 m^2/d at the right boundary and a sink of equal size at the left side. The layer has a length of 30 m and a height of 10 m. To the upper boundary of the layer an atmospheric pressure condition is imposed, all other boundaries are impermeable. Initially the lower half of the domain has a concentration 1 which corresponds to salt water with a density of 1025 kg/m^3. The upper half has a concentration 0 which corresponds to fresh water with a fluid density of 1000 kg/m^3. The permeability of the porous medium is 1 m/d, the dynamic viscosity is assumed to be constant and has a value of 10^{-3} Pas, the porosity is 0.4.

Figure 1 shows the results of a 2D simulation the dispersivities are α_l = 1 m, α_t = 0.5 m. Upconing takes place at the left side of the domain. The salt water zone is pushed down at the right size, however initially dispersion dominates convection and low concentrations are found upstream.

The results of a 2D simulation with a longitudinal dispersivity of 0.5 m and a transverse dispersivity of 0.1 m are shown in figure 2. For this case the brackish zone remains limited in size.

The results of the model are compared with the results of a sharp interface model. The result of the sharp interface model GAMMA [Verruijt 1996] are given in figure 3. This model is based on the same flow equation, fluid densities are kept constant for each element however.

Figure 4 displays a vertical section of a 3D model for longitudinal and transverse dispersivities of respectively α_l = 1 m, α_t = 0.5 m. The infiltration and abstraction rates are 0.33 m^3/d, the computational domain is extended in the third direction to 5 m. Upconing is less severe under these conditions as can be expected.

Finally the results of a decoupled simulation are presented in figure 5, dispersivities now are again α_l = 1 m, α_t = 0.5 m. For this simulation fluid density is assumed to be independent of the concentration. As a result of this, upconing will be greater; the driving force downward is not present.

Conclusions

For a sharp interface problem the time scale and length scale differ from a coupled convection-dispersion problem. Sharp interface models show less upconing at the same time, this is partially the result of the smaller density force at low concentrations that counteracts the abstraction force. For early time steps a decoupled convection-diffusion model for which the density effect is not part of the problem gives a better estimate than a sharp interface approach.

The finite element formulation demonstrated in this paper is suitable for solving density dependent groundwater flow problems. Three dimensional calculations however require a lot of internal computer memory and calculation times may be long. For the presented case of a strip of 30 meters long 10 meters high and 5 meters of with, 10 Mb memory was required an the calculation time was about 5 hours (on a 100 MHz Pentium PC) till the equilibrium state was almost reached at 1000 days. Comparing the results with the two dimensional simulation it must be noted that one has to be very careful in applying two dimensional models for a really three dimensional problem.

Coupled convection-diffusion problems with fresh water on top of a salt water zone, differ numerically from uncoupled convection-diffusion problems for transport of a pollutant. In zones where the convection is small, diffusion will be small too, the front remains steep giving rise to numerical oscillations. These oscillations may be suppressed by using a lumped mass formulation, however numeric simulations showed that the mesh size must be smaller than 5 times the lowest dispersivity coefficient (according to the Peclet number, the Courant number may be used to determine the time step size). The finite element method seems to be very efficient for three

dimensional modelling of groundwater flow problems, as it is possible to refine the mesh in parts of the computational domain where large gradients are expected.

To reduce calculation times and to limit memory requirements, an Arbitrary Lagrangian-Eulerian (ALE) description is proposed. Pressures and velocities will be calculated for a fixed Eulerian mesh. Soil parameters are kept constant within an element which seems physically right. Concentrations however will be calculated for a moving Lagrangian mesh, displacement of the mesh nodes account for the convection part of the transport equation. Local refinement of the mesh in the front between salt and fresh water may be necessary for reasons of accuracy.

Practically dispersion is dominated by variations in the convection field due to heterogenities in the soil properties and temporal variations in the boundary conditions. As these variations are unknown dispersion accounts for a statistical process. It is assumed that dispersion will be the main contributor to mixing and the development of the brackish zone, this process will be studied by physical models as well. Temperature effects might be important too, the model will be extended to account for these effects. A sensitivity study has to show which of the processes are most important for modelling an abstraction-infiltration problem. A faster model may be derived using this knowledge.

REFERENCES

Bathe K.J., 1996: Finite element procedures in engineering analysis, Prentice Hall, Englewood Cliffs.

Bear J., 1972: Dynamics of fluids in porous media, Dover Publications inc., New York.

Bear J., Verruijt A., 1987: Modelling groundwater flow and pollution, Reidel, Dordrecht.

Huyakorn P.S., Pinder G.F., 1983: Computational methods in subsurface flow, Academic Press, New York.

Press h.w., ea., 1988: Numerical recipes in C, 2d ed., Cambridge University Press, New York.

Verruijt A., 1996: Gamma, A computer model for interface flow, Delft University of technology, Delft.

Verruijt A., 1996: Displacement of an interface between fresh and salt groundwater, Delft.

Zienkiewics O.C., 1977: The finite element method, 3d ed., McGraw-Hill, London.

FIGURE 1, 2D simulation results (α_l = 1 m, α_t = 0.5 m)

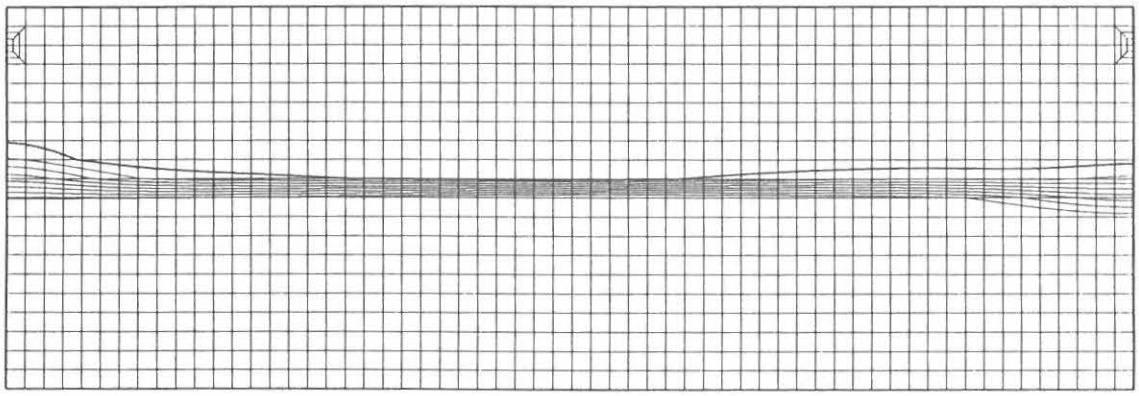

figure 1a, t = 10 days

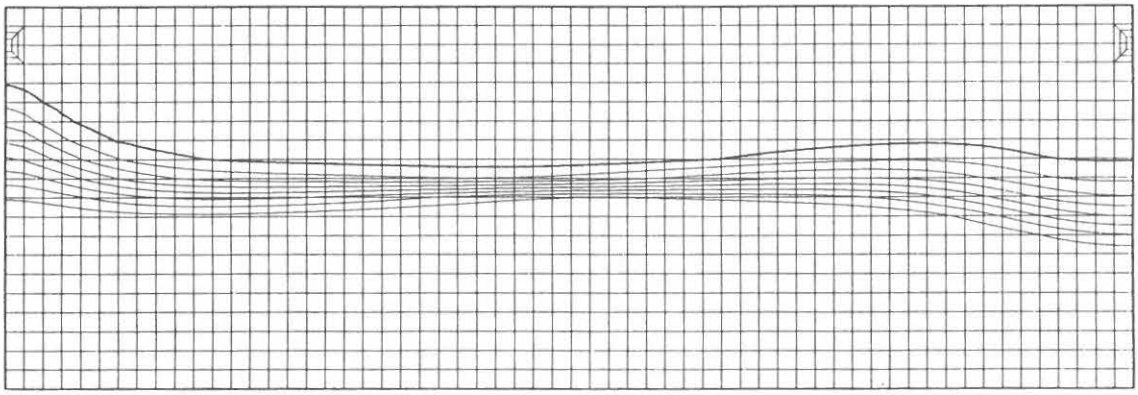

figure 1b, t = 50 days

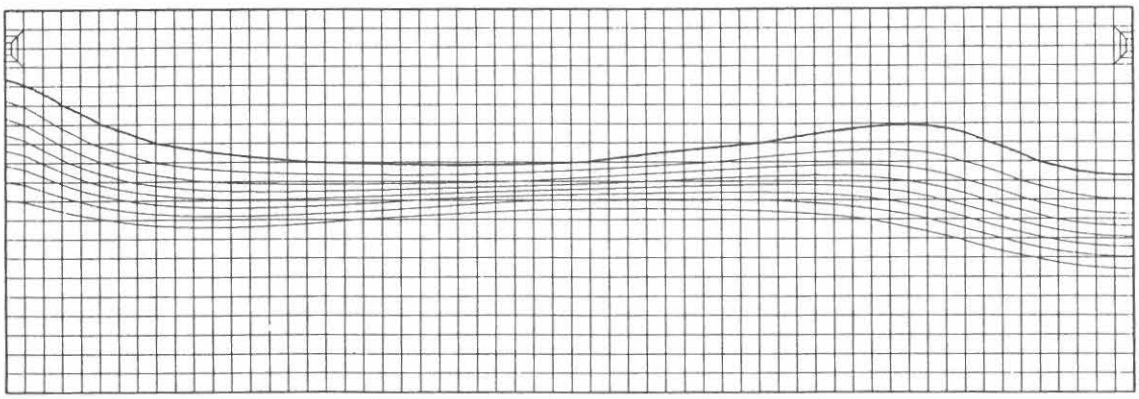

figure 1c, t = 100 days

FIGURE 2, 2D simulation results (α_l = 0.5 m, α_t = 0.1 m)

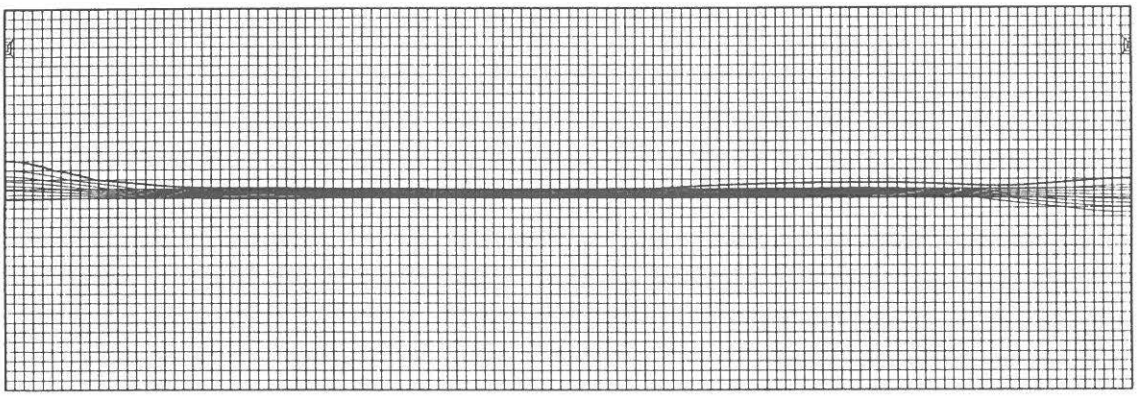

figure 2a, t = 10 days

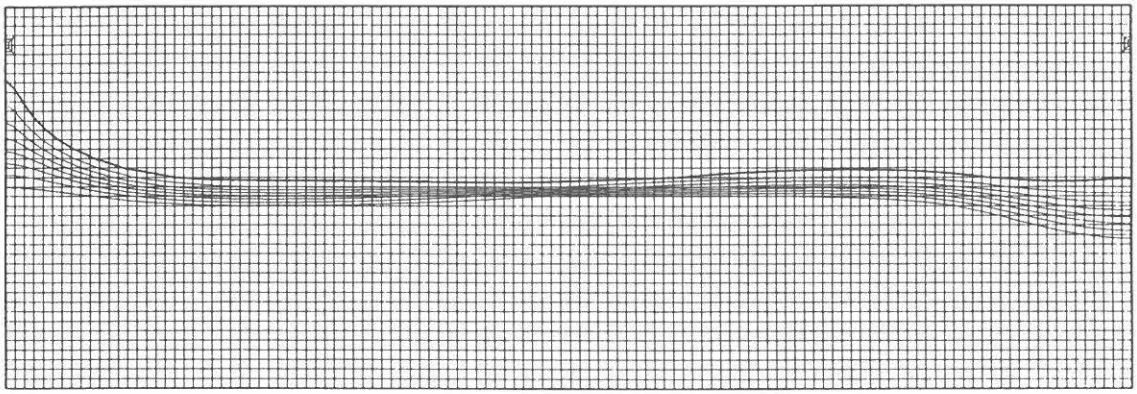

figure 2b, t = 50 days

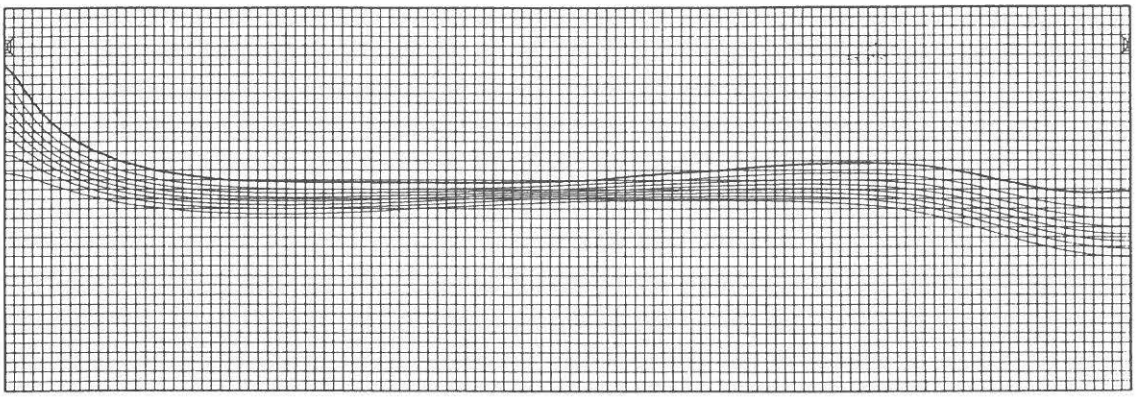

figure 2c, t = 100 days

FIGURE 3, 2D simulation results sharp interface model

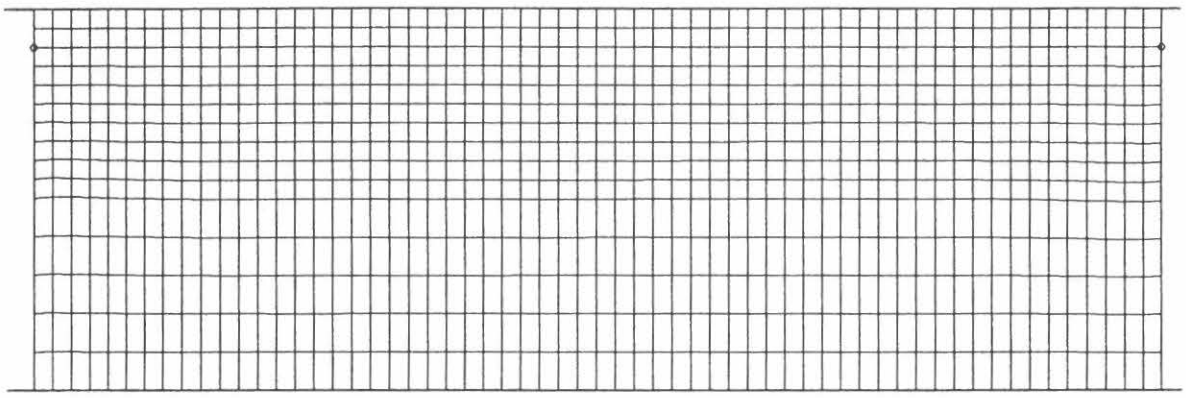

figure 3a, t = 10 days

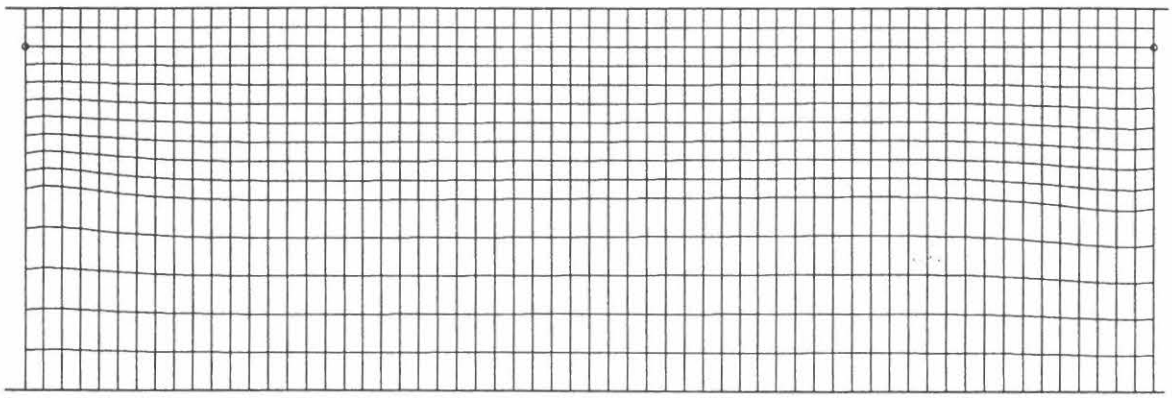

figure 3b, t = 50 days

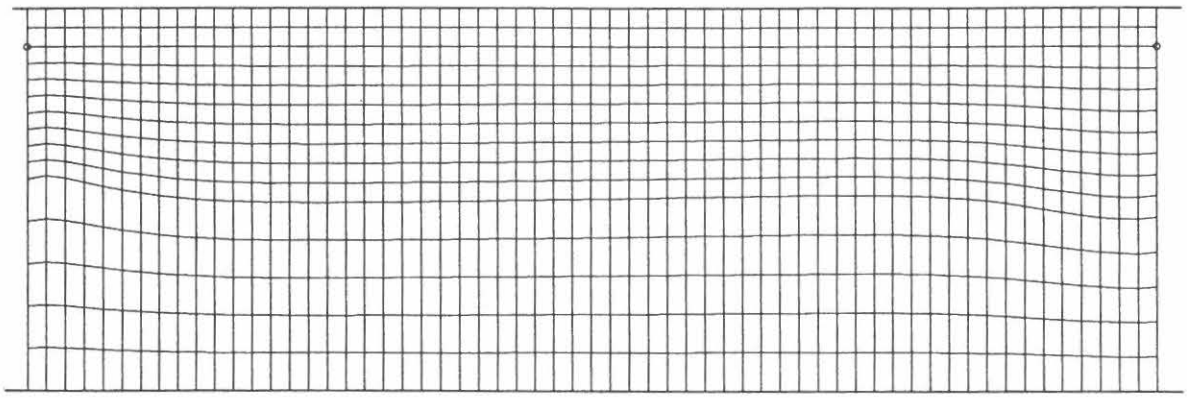

figure 3c, t = 100 days

FIGURE 4, 3D simulation results (α_l = 1 m, α_t = 0.5 m)

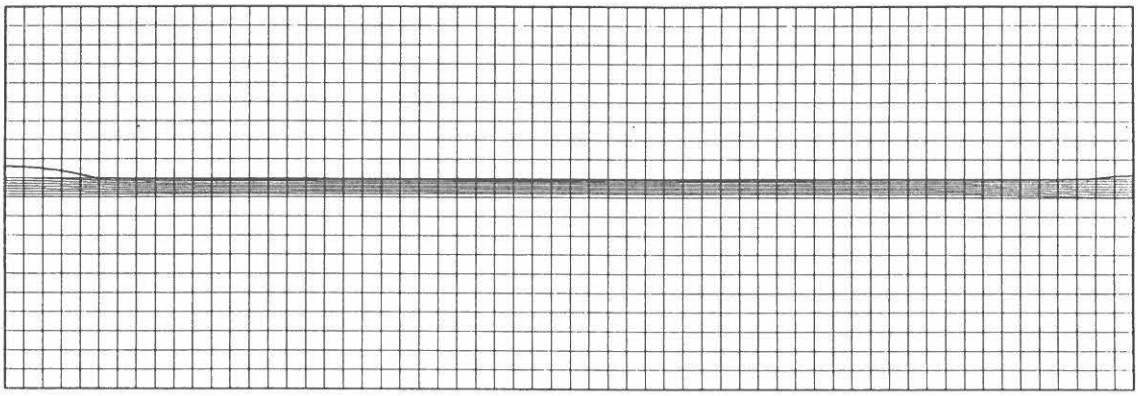

figure 4a, t = 10 days

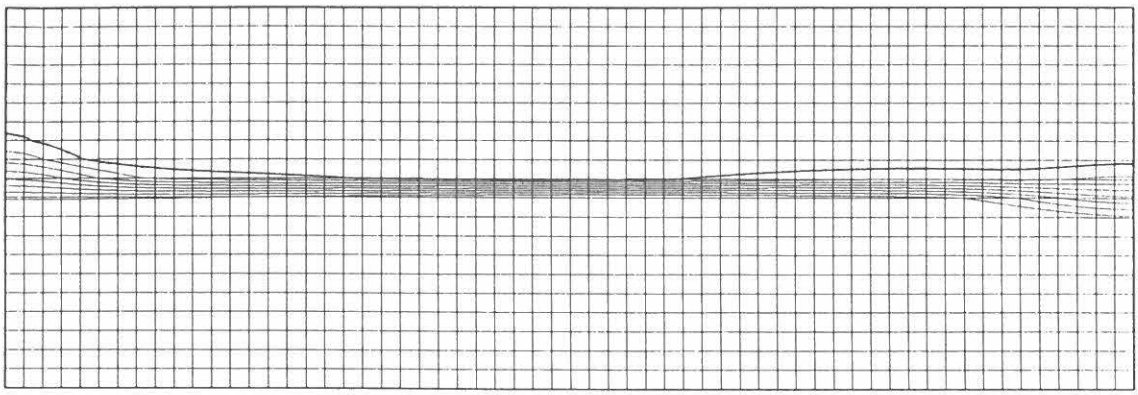

figure 4b, t = 50 days

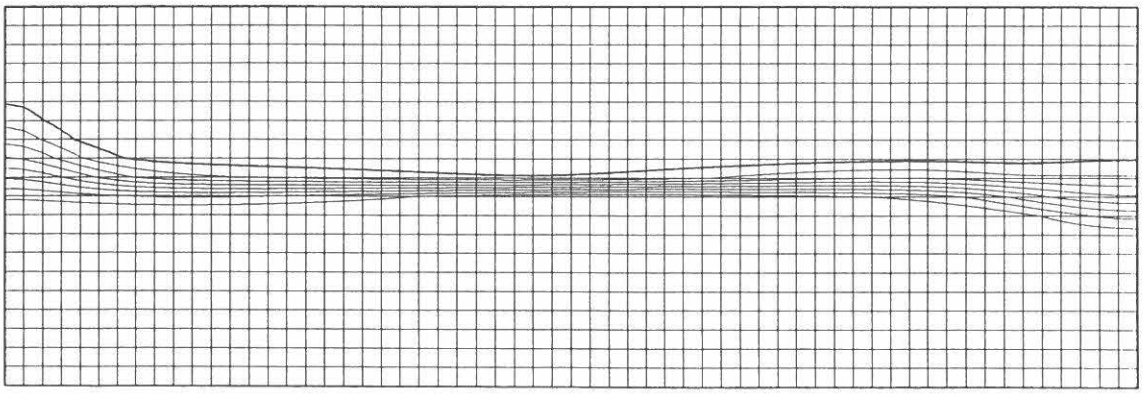

figure 4c, t = 100 days

FIGURE 5, 2D decoupled simulation results (α_l = 1 m, α_t = 0.5 m)

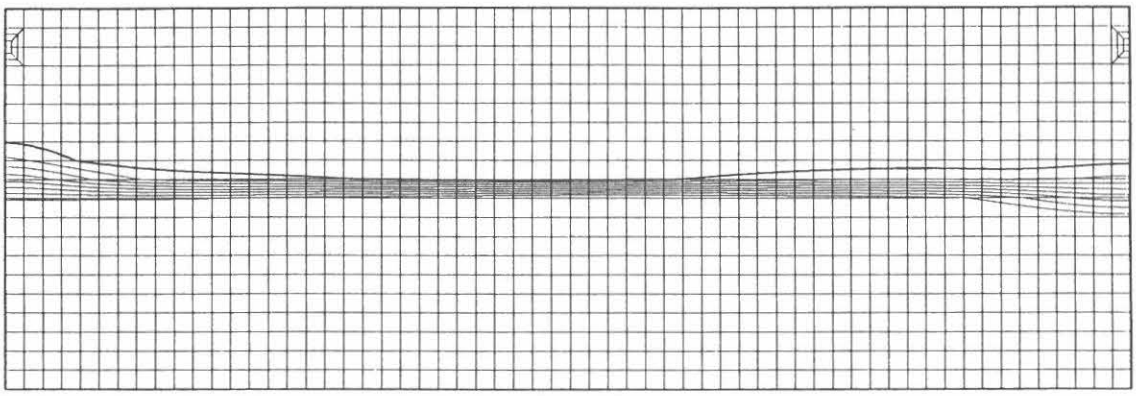

figure 5a, t = 10 days

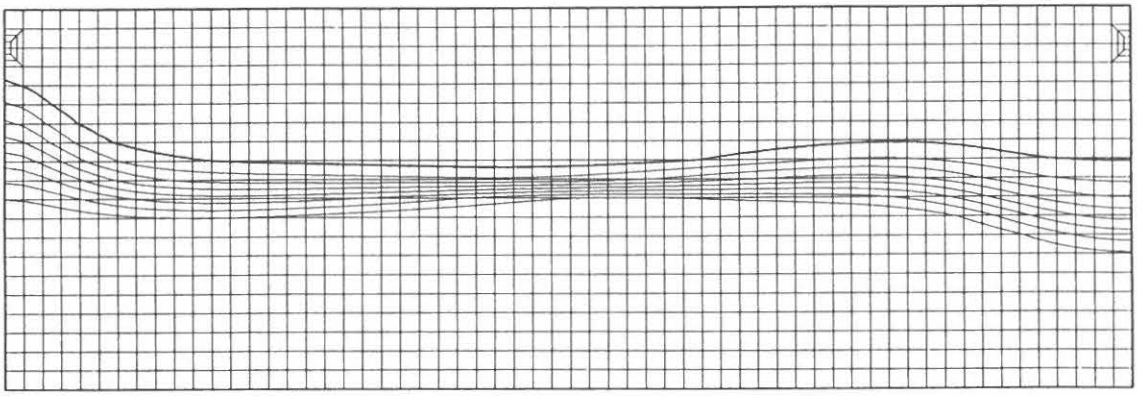

figure 5b, t = 50 days

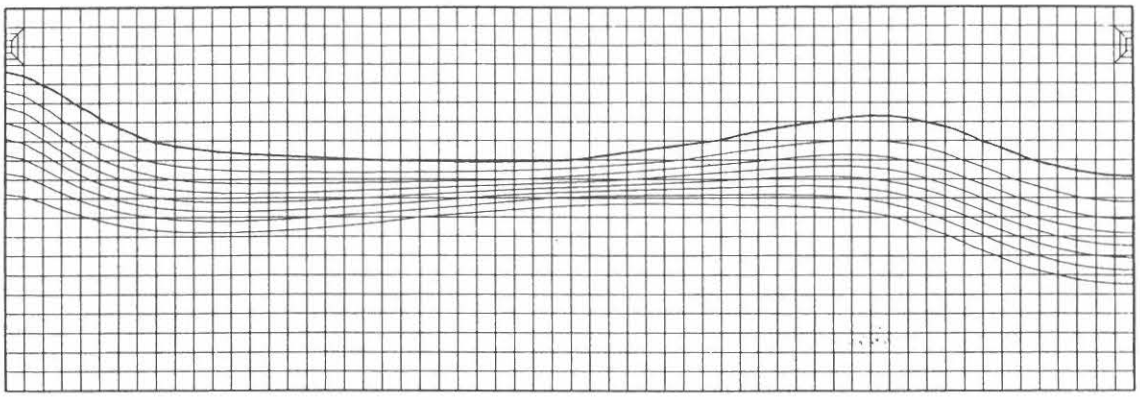

figure 5c, t = 100 days